Energy Engineering

Tech Science Press

https://doi.org/10.32604/ee.2026.073739

ARTICLE

Flexible Matching of Maximum Service Restoration Strategies in Active Distribution Networks

Yi An[1], **Litao Hong**[2], **Chun Chen**[3,*], **Zihan Zhang**[3] and **Yijia Cao**[3]

[1]Electric Power Science Research Institute of State Grid Jiangxi Electric Power Co., Ltd., Nanchang, China
[2]China Energy Engineering Group Hunan Electric Power Design Institute Co., Ltd., Changsha, China
[3]National Key Laboratory of Power Grid Disaster Prevention and Mitigation, Changsha University of Science and Technology, Changsha, China

*Corresponding Author: Chun Chen. Email: chch3266@126.com

Received: 24 September 2025; Accepted: 18 November 2025; Published: 30 August 2026

ABSTRACT: With the rapid development and widespread application of distributed energy resources (DERs), service restoration in the distribution network has become more complex and challenging. This paradigm shift, while offering unprecedented opportunities for a cleaner and more resilient energy grid, has fundamentally altered the traditional, centralized approach to managing power outages. This paper addresses the issue that intentional islanding partition and network reconfiguration are not effectively integrated during service restoration, proposing a flexible matching method for maximizing service restoration in the active distribution network. Firstly, a fault branch variable based on the basic ring matrix of the distribution network is proposed. The fault restoration strategy is then determined using the decision tree presented in this paper, and different objective functions are formulated for various fault strategies. Secondly, photovoltaic (PV) units and Wind Turbines (WTs), emergency electric vehicles (EEVs), energy storage systems (ESSs), and controllable loads are analyzed and modeled for their output characteristics in service restoration by considering the participation of DERs. Then, considering the non-convexity in controllable loads and power flow constraints, relaxation techniques are applied to transform the problem into a mixed-integer second-order cone programming (MISOCP) model for the solution. Finally, case studies are conducted on the IEEE 69-bus and IEEE 33-bus systems to verify the effectiveness of the proposed model and method.

KEYWORDS: Intentional islanding partition; network reconfiguration; faulted branch variable; MISOCP planning; distributed energy resources

1 Introduction

The integration of distributed generations (DGs) into traditional distribution networks has transformed them into multi-source distribution networks [1–3], and the extensive integration of various DGs has inevitably triggered fundamental changes in the topology of the distribution network. Consequently, traditional service restoration strategies are no longer applicable, and the restoration process has become more complex and challenging [4,5].

Currently, scholars have conducted extensive research on service restoration strategies for active distribution networks. Among these strategies, intentional islanding partition and network reconfiguration are two common approaches to restoration strategies [6]. Regarding intentional islanding partition, reference [7] employs the emergency black-start capability of DGs to form predefined islands that restore power to critical loads. Although this method ensures the power supply to important loads, it imposes high operational requirements on the islands. In reference [8], when partitioning islands, the number of DGs is set equal to the number of islands, which sacrifices the possibility of merging multiple islands and thereby prevents the formulation of an optimal service restoration strategy. In terms of algorithm selection, traversal methods commonly used for intentional islanding partition in distribution networks with DGs are mostly based on graph theory. Such methods initially simplify the distribution networks model into a graph and then utilize graph theory techniques for intentional islanding partition [9]. In reference [10], a heuristic rule is proposed to selectively add loads to the island, restoring a greater amount of load within its range. In reference [11], an optimization strategy based on mixed-integer linear programming is proposed, aiming to reduce the curtailment of critical loads in islands. In reference [12], the uncertainty of DG output is considered. And introducing auxiliary variables and applying convex relaxation, the model is transformed into a mixed-integer quadratic-constrained programming model and solved. For network reconfiguration, current research on network reconfiguration methods in distribution networks mainly include heuristic algorithms, intelligent optimization algorithms, and mathematical programming [13,14]. An improved heuristic algorithm is proposed to perform network reconfiguration with the objective of minimizing network losses in reference [15]. In reference [16], a genetic algorithm is proposed to solve the network reconfiguration problem. All switches in the distribution networks are encoded in a binary manner (0 or 1). However, due to the neglect of the characteristics of distribution networks, a large number of infeasible solutions are contained in the generated initial solutions, which reduces the algorithm's solving speed. In reference [17], an improved "destruction" particle swarm optimization algorithm is employed for the restoration of distribution networks, which enhances the algorithm's accuracy, convergence speed, and stability. In reference [18], two new network reconfiguration optimization models for mathematical programming are proposed, which are mixed-integer linear programming (MILP) and mixed-integer conic programming (MICP).

Many studies combine intentional islanding partition and network reconfiguration to achieve improved restoration results. In reference [19], the islands are predefined based on the capacity and type of DGs, as well as the importance level of the loads. After a fault occurs, the DGs in the power outage area that can operate independently run under predefined conditions. Then, the remaining network area outside the islands is reconfigured to restore the power supply. However, this method fails to fully integrate intentional islanding partition with network reconfiguration. In reference [20], a service restoration strategy that comprehensively integrates intentional islanding partition and network reconfiguration is proposed, and the influence of tie switches in the intentional islanding partition process is examined. Furthermore, a unified service restoration model for intentional islanding partition and network reconfiguration in distribution networks is proposed in reference [21], which partially addresses the coordination issue between these two methods.

Meanwhile, the integration of distributed energy resources (DERs), such as DGs, emergency electric vehicles (EEVs), energy storage systems (ESSs), and controllable loads provides new opportunities and challenges for the restoration of distribution networks [22,23]. In reference [20], the impact of DGs on distribution network restoration is considered, but the issue of DG output uncertainty is not addressed. Building upon the previous work, reference [24] takes the uncertainty of DG output into account and proposes a robust optimization model to determine the optimal configuration under worst-case scenarios. The results indicate that although considering the uncertainty of DG output reduces the load recovery capability, it provides greater robustness. In references [25–27], the impacts of EEVs, EESs, and controllable loads on service restoration are explored. Case studies show that the integration of these DERs can significantly enhance load recovery capability.

Regarding the aforementioned research, this study proposes a flexible matching method for maximum power supply restoration strategy in active distribution networks with faults. The main contributions of this paper are as follows:

(1) Based on the basic ring matrix, the faulted branch variable and a service restoration decision tree are proposed. When faults occur, the faulted branch variable is calculated using the basic ring matrix, and the service restoration strategy is determined based on the decision tree.

(2) Models for the intentional islanding partition and network reconfiguration service restoration strategies are respectively established. According to the emphasis of each strategy, corresponding objective functions and constraints are set, and the output characteristics of DERs in the model are analyzed. Subsequently, the service restoration model is linearized using second-order cone relaxing techniques and the McCormick relaxation method.

2 Article Framework

This study is organized into three main parts. In the first part, a detailed overview of service restoration strategy types is provided. In addition, a faulted branch variable and a service restoration decision tree are introduced to determine the appropriate restoration strategy for the power outage area, and models for various service restoration strategies are established. The second part analyzes the output characteristics of DERs and models them for integration into the distribution network. In the third part, the service restoration model, originally formulated as a nonlinear programming problem, is transformed into a mixed-integer second-order cone programming (MISOCP) problem to be solved. Fig. 1 illustrates the overall framework and methodology of the proposed service restoration method.

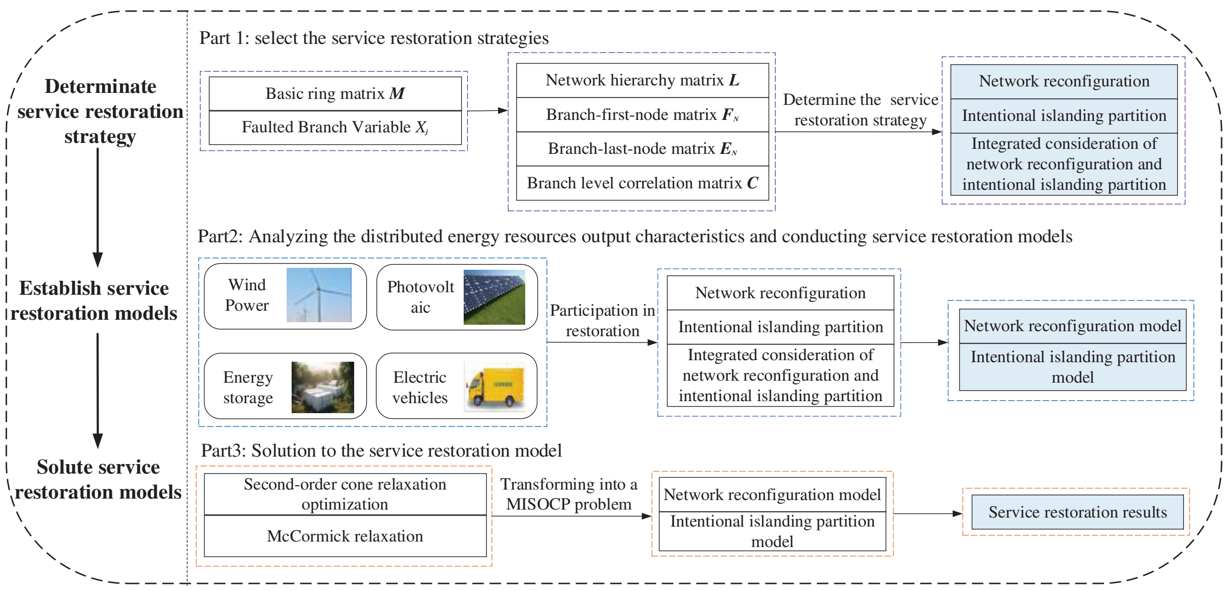

Figure 1: The overall architecture of the service restoration method proposed in this paper

3 Service Restoration Model

Due to the prominent advantages of DGs, multi-source distribution networks have become an inevitable trend. For distribution networks containing DGs, intentional islanding partition and network reconfiguration are the two main service restoration strategies. In this chapter, the service restoration strategy is determined by using a faulted branch variable and a service restoration decision tree, and models for service restoration strategies that incorporate intentional islanding partition and network reconfiguration with the participation of DERs are established.

3.1 Service Restoration Strategy

Fig. 2a shows the initial topology. When faults occur in the distribution network, the restoration strategy of faulty power outage areas can be categorized into the following three modes:

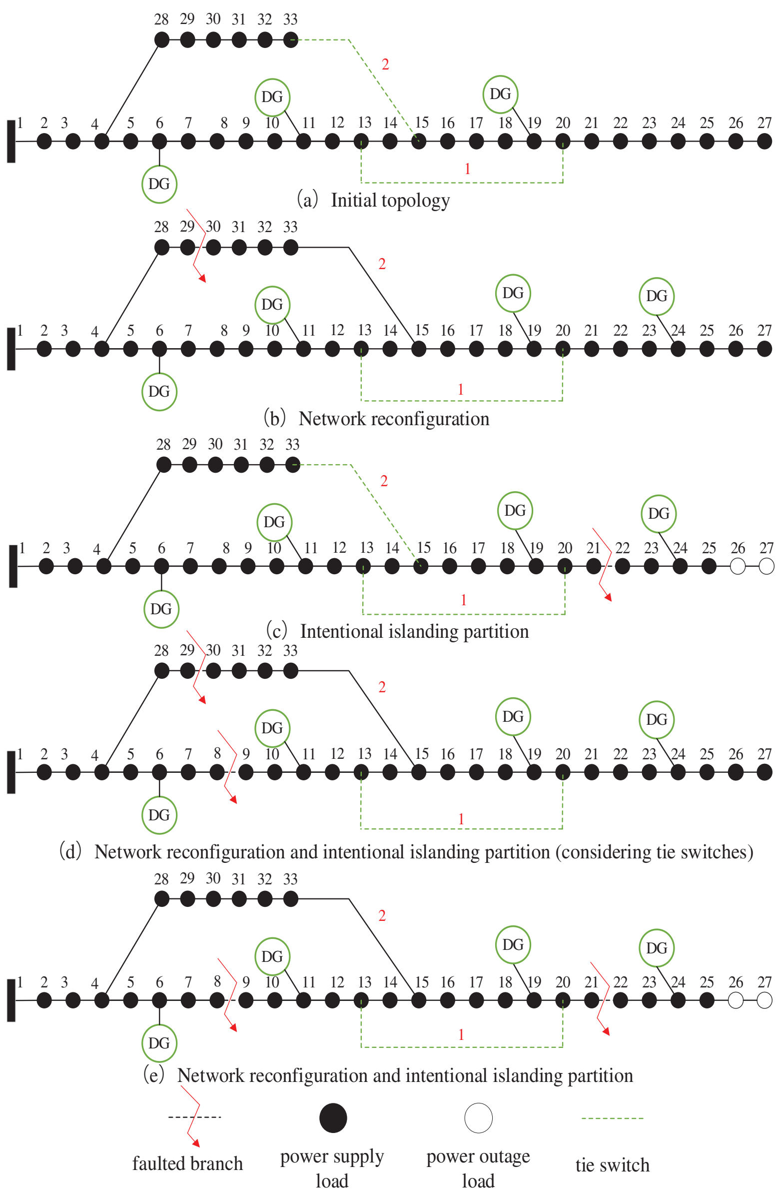

Figure 2: Service restoration strategies of distribution network

(1) Network reconfiguration mode (restoring power supply by switching the statuses of tie and sectional switches): The fault between nodes 29 and 30 causes a power outage area from nodes 30 to 33, which can be restored by closing the tie switch (see Fig. 2b).

(2) Intentional islanding partition mode (restoring power supply by using DGs): The fault between nodes 21 and 22 causes an outage from nodes 22 to 27, which can be restored by using the DGs at node 24 (see Fig. 2c).

(3) Combined intentional islanding partition and network reconfiguration mode (using tie switches to expand island areas and increase the recovery load): As shown in Fig. 2a, a fault between nodes 8 and 9 and between nodes 29 and 30 causes a power outage area from nodes 9 to 33. By closing tie switch 2, the power supply is restored to nodes 9 to 33 (see Fig. 2d). Similarly, a fault between nodes 8 and 9 and between nodes 21 and 22 causes a power outage from nodes 9 to 27. In this case, nodes 22 to 27 form an island area powered by the DG at node 24, while nodes 9 to 21 are restored by closing tie switch 2 (see Fig. 2e).

In the above three service restoration modes, the latter one is both combinations of intentional islanding partition and network reconfiguration, which have been a major focus of research in recent years. For restoring power to outage areas, this paper prioritizes using network reconfiguration to power supply, since it provides more stable power supply compared with the islanding partition approach. If restoration by network reconfiguration is not feasible, the next option is to form islands for power supply restoration based on DGs. Mathematically, the model of service restoration that combines intentional islanding partition and network reconfiguration is a multi-objective, multi-constraint nonlinear integer programming problem.

3.2 Service Restoration Strategy Selection

After faults occur, it is crucial to quickly determine the appropriate service restoration strategy. Based on the basic ring matrix and faulted branch variable, this paper proposes a decision tree and further integrates intentional islanding partition and network reconfiguration.

In a radial distribution network, a ring formed by a tie switch and several sectional switches is referred to as a basic ring. The definition and construction steps of the basic ring matrix M are described in reference [28]. Taking the wiring diagram of node 69 in Fig. 3 as an example, the basic ring matrix M is as follows:

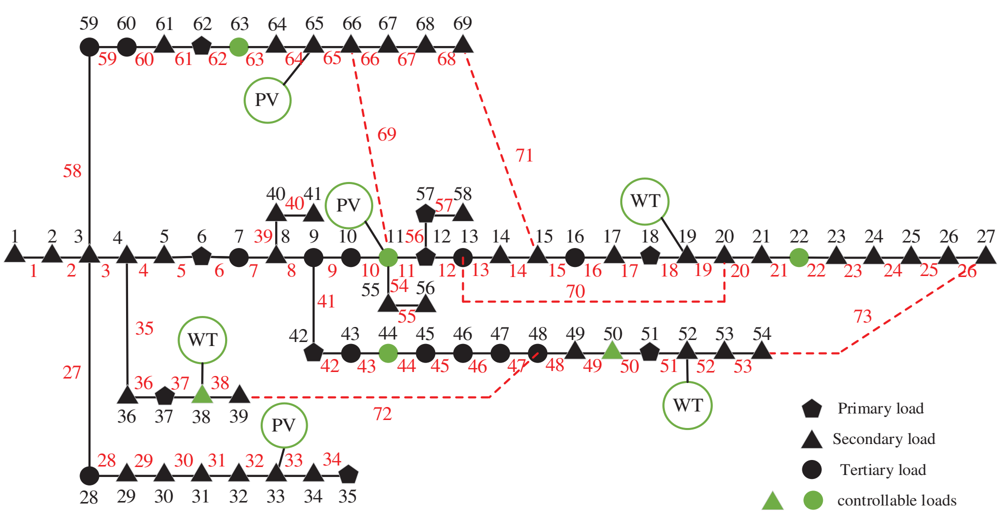

Figure 3: 69-bus distribution network system

$$M = \begin{bmatrix} 3 & 4 & 5 & 6 & 7 & 8 & 9 & 10 & 58 & 59 & 60 & 61 & 62 & 63 & 64 & 65 & 0 & 0 & 0 & 0 & 0 & 0 & 0 & 0 & 0 & 0 & 0 & 0 & 0 & 0 & 0 \\ 13 & 14 & 15 & 16 & 17 & 18 & 19 & 0 & 0 & 0 & 0 & 0 & 0 & 0 & 0 & 0 & 0 & 0 & 0 & 0 & 0 & 0 & 0 & 0 & 0 & 0 & 0 & 0 & 0 & 0 & 0 \\ 3 & 4 & 5 & 6 & 7 & 8 & 9 & 10 & 11 & 12 & 13 & 14 & 58 & 59 & 60 & 61 & 62 & 63 & 64 & 65 & 66 & 67 & 68 & 0 & 0 & 0 & 0 & 0 & 0 & 0 & 0 \\ 4 & 5 & 6 & 7 & 8 & 35 & 36 & 37 & 38 & 41 & 42 & 43 & 44 & 45 & 46 & 47 & 0 & 0 & 0 & 0 & 0 & 0 & 0 & 0 & 0 & 0 & 0 & 0 & 0 & 0 & 0 \\ 9 & 10 & 11 & 12 & 13 & 14 & 15 & 16 & 17 & 18 & 19 & 20 & 21 & 22 & 23 & 24 & 25 & 26 & 41 & 42 & 43 & 44 & 45 & 46 & 47 & 48 & 49 & 50 & 51 & 52 & 53 \end{bmatrix}$$

This paper introduces the faulted branch variable x_l^a and employs the service restoration decision tree to determine the service restoration strategy after faults occur. The definition of the faulted branch variable x_l^a is given by:

$$x_l^a \in \{0,1\}, \quad a \in A, l \in \Omega_l \tag{1}$$

where, x_l^a is faulted branch variables; $x_l^a = 1$ indicates that branch l is part of the a-th basic ring; $x_l^a = 0$ indicates that branch l is not part of the a-th basic ring; A is set of basic ring sets in distribution network system; Ω_l is set of branches in distribution network.

Based on the faulted branch variable, a decision tree is used to guide the selection of service restoration strategies. The decision tree features include the number of faulted branches, the faulted branch variables, and the presence of tie switches. The specific steps are as follows:

(1) Root node: Number of faulted branches.

When there is one faulted branch, Judgment One is applied. When there are two faulted branches, Judgment Two is applied. When there are three or more faulted branches, Judgment Three is applied.

(2) Lead node one: Faulted branch variables.

Judgment One:

If $\sum_{a=1}^{A} x_l^a = 0$, it indicates that the faulted branch occurred outside the basic ring matrix, so the intentional islanding partition service restoration strategy is adopted.

If $\sum_{a=1}^{A} x_l^a \geq 1$, it indicates that the faulted branch occurred within the basic ring matrix, and therefore, the network reconfiguration service restoration strategy is adopted.

Judgment Two:

If $\sum_{a=1}^{A} x_n^a = 0$ and $\sum_{a=1}^{A} x_m^a \geq 1$, the intentional islanding partition service restoration strategy is adopted.

If $\sum_{a=1}^{A} x_n^a \geq 1$ and $\sum_{a=1}^{A} x_m^a = 0$, the combined strategy of intentional islanding partition and network reconfiguration is adopted, with intentional islanding partition applied to the area outside the basic ring and network reconfiguration applied to the area within the basic ring.

If $\sum_{a=1}^{A} x_n^a = \sum_{a=1}^{A} x_m^a = 1$, and $\forall a, x_n^a = x_m^a$, the intentional islanding partition service restoration strategy is adopted.

If $\sum_{a=1}^{A} x_n^a = \sum_{a=1}^{A} x_m^a \geq 2$, and $\forall a, x_n^a = x_m^a$, the combined strategy of intentional islanding partition and network reconfiguration is adopted, with intentional islanding partition and network reconfiguration applied to each area.

If $\sum_{a=1}^{A} x_n^a \geq 1$, $\sum_{a=1}^{A} x_m^a \geq 1$, and $\exists a, x_n^a \neq x_m^a$, then the network reconfiguration service restoration strategy is used.

Judgment Three:

The service restoration strategy can be obtained by arranging and combining the fault situations of one or two faulted branches.

(3) Leaf node two: Presence of tie switches.

If the intentional islanding partition strategy is used for the above scenarios, it is necessary to determine whether tie sitches exist within the faulty power outage area. If they do, the impact of the tie switches on the intentional islanding partition process should be considered; otherwise, no further consideration is required.

The decision tree for the service restoration strategy is shown in Fig. 4. The corresponding basis for the judgment is shown in Table 1.

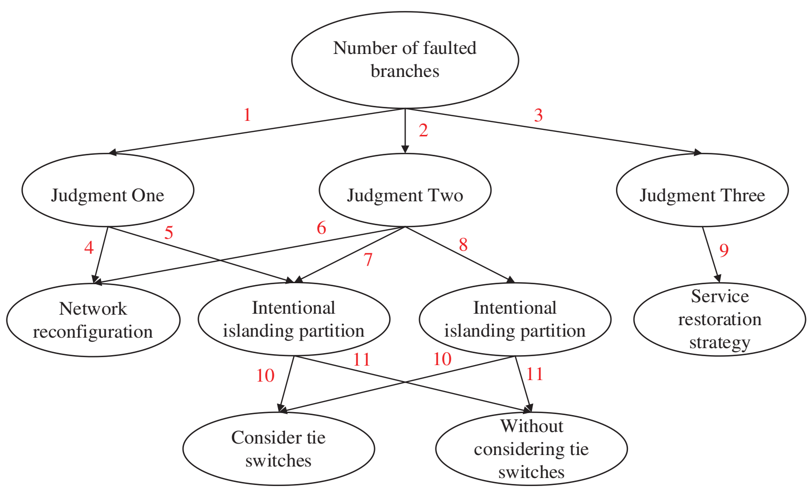

Figure 4: The decision tree for service restoration strategy

Table 1: The corresponding basis for the judgment

Directed edge number	The basis for the judgment
1	One faulted branch
2	Two faulted branches
3	Three or more faulted branches
4	$\sum_{a=1}^{A} x_l^a = 0$
5	$\sum_{a=1}^{A} x_l^a \geq 1$
6	$\sum_{a=1}^{A} x_n^a \geq 1$, $\sum_{a=1}^{A} x_m^a \geq 1$, and $\exists a, x_n^a \neq x_m^a$

(Continued)

Table 1 (continued)

Directed edge number	The basis for the judgment
7	$\sum_{a=1}^{A} x_n^a = 0,\ \sum_{a=1}^{A} x_m^a = 0;\ \sum_{a=1}^{A} x_n^a = \sum_{a=1}^{A} x_m^a = 1$, and $\forall a, x_n^a = x_m^a$
8	$\sum_{a=1}^{A} x_n^a \geq 1,\ \sum_{a=1}^{A} x_m^a = 0; \sum_{a=1}^{A} x_n^a = \sum_{a=1}^{A} x_m^a \geq 2$, and $\forall a, x_n^a = x_m^a$
9	Combination of Judgment One and Two
10	There are tie switches within the faulty power outage area
11	There are no tie switches within the faulty power outage area

3.3 Service Restoration Model

Once the restoration strategy is determined, both intentional islanding partition and network reconfiguration require that the faulty power outage areas be identified in advance. The faulty power outage areas of the distribution network are solely determined by the topology of the distribution network. Once the structure of the distribution network is determined, the faulty power outage areas of the distribution network are uniquely determined.

The hierarchical approach for distribution network topology is as follows: the feeders, outgoing lines, and busbars are considered as the first-level nodes. Then, a traversal is performed in the direction of the terminal branches to identify the subsequent-level branches, thereby establishing a parent-child relationship between upper and lower nodes. This process continues until all branches have been explored, resulting in the generation of the network's hierarchical matrix L, branch node matrices FN and EN, and branch branch-level correlation matrix C [29].

3.4 Determining the Faulty Power Outage Areas

After determining the service restoration strategy for the power system and identifying the faulty power outage areas, it is necessary to model each service restoration strategy to achieve effective fault handling. This study focuses on the mathematical modeling of two strategies: intentional islanding partition and network reconfiguration.

3.4.1 Network Reconfiguration

The objective function under the network reconfiguration strategy is given by:

$$f = \min \sum_{\forall l_{ij} \in \Omega_l} r_{ij} I_{ij}^2 + \sum_{\forall i \in \Omega_n} |U - U_i| \tag{2}$$

where, r_{ij} is resistance of branch ij; I_{ij} is current through branch ij; U is reference voltage; U_i is voltage value at node i; Ω_n is set of nodes in distribution network.

As demonstrated in Eq. (3), the three sub-objective functions exhibit distinct dimensions and units. To enable their summation, each function must undergo linear normalization prior to aggregation, thereby transforming all data into the [0, 1] interval. The specific implementation procedure is as follows:

$$X_{\text{norm}} = \frac{X - X_{\min}}{X_{\max} - X_{\min}} \tag{3}$$

where, X_{norm} is the normalized value of each sub-objective function; X is the sub-objective function value after iteration completion; X_{min} is the minimum sub-objective function values; X_{max} is the maximum sub-objective function values.

The constraints include:

(1) EEV configuration constraint. The constraint on EEV configuration is defined based one Eq. (4).

$$\begin{cases} \sum\limits_{c \in C} z^{ci} \le 1, & \forall i \in \Omega_n \\ \sum\limits_{i \in \Omega_n} z^{ci} = 1, & \forall c \in C \end{cases} \tag{4}$$

where, $z^{ci} = 1$ indicates that EEV c is connected to node i, while $z^{ci} = 0$ indicates that EEV c is not connected to node i; C is set of EEV. The first line of Eq. (4) indicates that at most one EEV can be connected to each node. The second line of Eq. (4) indicates that each EEV can only be connected to one node.

(2) Radiality constraint. The branch status variable in the distribution network is matched with the number of branches and the relationship between tie switches as described in Eq. (5).

$$\begin{cases} \sum\limits_{(ij) \in \Omega_l} z_{ij} = n_b - n_s \\ z_{ij} \in \{0,1\}, \forall (ij) \in \Omega_l \end{cases} \tag{5}$$

$$\sum_{(ij) \in C_a} z_{ij} \le |C_a| - 1, \forall C_a \in \mathcal{B}. \tag{6}$$

where, z_{ij} is branch ij switch status variable; n_b is total number of nodes in the distribution network; n_s is total number of root nodes in the distribution network; $\mathcal{B}$ is the fundamental cycle set; C_a denotes the a-th fundamental cycle; $|C_a|$ is the number of branches in C_a.

(3) Power flow constraints. Based on reference [30], the power flow constraints for multi-source distribution networks are defined based on Eqs. (7)–(12).

$$\sum_{j \in \phi(i)} P_{ji} - \sum_{k \in \phi(i)} P_{ik} - r_{ji} I_{ji}^2 = P_i \tag{7}$$

where, P_{ji} is active power transmitted from node j to node i; P_{ik} is active power transmitted from node i to node k; $\phi(i)$ is set of upstream nodes connected to node i; P_i is Net injected active power at node i.

$$\sum_{j \in \phi(i)} Q_{ji} - \sum_{k \in \phi(i)} Q_{ik} - x_{ji} I_{ji}^2 = Q_i \tag{8}$$

where, Q_{ji} is reactive power transmitted from node j to node i; Q_{ik} is reactive power transmitted from node i to node k; Q_i is Net injected reactive power at node i.

$$P_i = (-r_i \beta_i P_{Load,i} + P_{Load,i}) - P_i^{WT} - P_i^{PV} - P_i^{eev} - P_i^{ess} \tag{9}$$

where, r_i is adjustment ratio of adjustable load; β_i is load connection variables; $P_{Load,i}$ is active load at node i; P_i^{WT} is active power generated by WT at node i; P_i^{PV} is active power generated by PV at node i; P_i^{eev} is active power of EEV at node i; P_i^{ess} is active power of ESS at node i.

$$Q_i = (-r_i \beta Q_{Load,i} + Q_{Load,i}) - Q_i^{WT} - Q_i^{PV} - Q_i^{eev} - Q_i^{ess} \tag{10}$$

where, $Q_{Load,i}$ is reactive load at node i; Q_i^{WT} is reactive power generated by WT at node i; Q_i^{PV} is reactive power generated by PV at node i; Q_i^{eev} is reactive power of EEV at node i; Q_i^{ess} is reactive power of ESS at node i.

$$I_{ij}^2 = \frac{P_{ij}^2 + Q_{ij}^2}{U_i^2} \tag{11}$$

$$U_i^2 - U_j^2 - 2\left(r_{ij}P_{ij} + x_{ij}Q_{ij}\right) + \left(r_{ij}^2 + x_{ij}^2\right) I_{ij}^2 = 0 \tag{12}$$

where, x_{ij} is intentional islanding partition variable of the branch of the branch ij, $x_{ij} = 1$ indicates that branch ij belongs to the island, while $x_{ij} = 0$ indicates that branch ij does not belong to the island.

(4) Safety operation constraints. Branch capacity constraint, voltage constraint, and current constraint are also introduced into the network reconfiguration model.

$$|P_l| \le P_{l\max} \tag{13}$$

where, $|P_l|$ is active power of the branch l; $P_{l\max}$ is maximum capacity of the branch l.

$$U_{\min}^2 \le U_i^2 \le U_{\max}^2 \tag{14}$$

where, $U_{\min}$ is minimum voltage value at node i; $U_{\max}$ is maximum voltage value at node i.

$$0 \le I_{ij}^2 \le z_{ij} I_{\max}^2 \tag{15}$$

where, $I_{\max}$ is maximum current through branch ij.

3.4.2 Intentional Islanding Partition

The objective function under the intentional islanding partition strategy is given by:

$$\begin{aligned} f &= \max\left[\sum_{\forall i \in C_L} \left(-r_i\beta_i P_{\mathrm{Load},i} + P_{\mathrm{Load},i}\right) w_i v_i + \sum_{\forall j \in C_L} r_j y_j w_j P_{\mathrm{Load},j}\right] \\ &= \min\left[\sum_{\forall i \in C_L} w_i \left(-r_i\beta_i y_i P_{\mathrm{Load},i} + y_i P_{\mathrm{Load},i}\right) - \sum_{\forall j \in C_L} r_j y_j w_j P_{\mathrm{Load},j}\right] \end{aligned} \tag{16}$$

where, $y_j = 1$ is charge state of node i; $y_j = 1$ indicates that the load is powered, while $y_j = 0$ indicates that the load is in an outage state; w_i is weight corresponding to load node i.

The Constraints include:

(1) EEV configuration constraint. Each EEV must be connected to nodes within the island, as described in Eq. (17).

$$\begin{cases} y_i \ge z^{ci}, & \forall i \in \Omega_n, \quad c \in C \\ z^{ci} \in \{0,1\}, & \forall i \in \Omega_n, \quad c \in C \end{cases} \tag{17}$$

(2) Intentional islanding partition constraint. When a line ij belongs to a certain island, the nodes i and j at both ends of the line must also belong to the same island, as expressed in Eqs. (7) and (18), among them, Eq. (18):

$$\begin{cases} x_{ij} = y^i y^j, & \forall ij \in \Omega_l \\ x_{ij} \in \{0,1\}, & \forall ij \in \Omega_l \end{cases} \tag{18}$$

(3) Radial constraint. The radial constraint for intentional islanding partition primarily considers the relationship between the number of restored loads and the number of islands.

$$\sum_{(ij)\in\Omega_l} x_{ij} \le n_b - s \tag{19}$$

where, s is number of islands in the island region.

(4) Power balance constraint. The total active power output from WT, PV, ESS, and EEV should exceed the total load demand within each island, as expressed in Eq. (20)

$$\sum_{i\in V_s} P_{Gi} > \sum_{j\in V_s} P_{Lj} \tag{20}$$

where, $\sum_{i\in V_s} P_{Gi}$ is total active power output of all DGs, ESS, and EEVs in island V_s; $\sum_{j\in V_s} P_{Lj}$ is total active power demand of all loads in island V_s.

(5) Power flow constraints. Variable r_i is introduced into constraints (9) and (10), leading to Eqs. (21) and (22):

$$P_i = (-r_i\beta_i P_{\text{Load},i} + P_{\text{Load},i})\, y_i - P_i^{\text{WT}} - P_i^{\text{PV}} - P_i^{\text{eev}} - P_i^{\text{ess}} \tag{21}$$

$$Q_i = (-r_i\beta_i Q_{\text{Load},i} + Q_{\text{Load},i})\, y_i - Q_i^{\text{WT}} - Q_i^{\text{PV}} - Q_i^{\text{eev}} - Q_i^{\text{ess}} \tag{22}$$

Other constraints are the same as those in the network reconfiguration model.

3.4.3 Load Shedding Operation

During network reconfiguration for service restoration, the voltage at the end of the branch may not meet the required voltage constraints, necessitating further load shedding operations. The specific load shedding steps are as follows:

(1) Marking and sorting adjustable loads: Mark the adjustable loads in the distribution network that have not yet been adjusted, and sort these nodes in ascending order based on their capacities to obtain a set of adjustable load points.

(2) Adjusting loads for constraint verification: In the set of adjustable loads, start adjusting from the load with the smallest adjustable capacity. After each adjustment, perform a power flow calculation for the distribution network to determine whether the voltage constraint conditions are met. If they are met, proceed to step (5); if not, move on to step (3).

(3) Marking loads to be shed: Select the node with the lowest voltage after network reconfiguration and mark the loads starting from the farthest end. Based on their importance, obtain a set of loads to be shed. Assign corresponding weights to different levels of loads, and determine the load shedding priority by multiplying the load size by its weight.

(4) Load shedding: First, shed the load at the farthest end, and then shed loads connected to it based on their priority. After each shedding, determine whether the voltage constraints are satisfied. If they are met, proceed to step (5); if not, continue shedding loads.

(5) Handling nodes with incomplete power supply recovery: Mark all load points that have been shed as nodes without completed power supply recovery. If any of these nodes are connected to DGs or are located within the islanded faulty power outage areas, include the load in the intentional islanding partition of the islanded area. If not, output the final service restoration result.

Through the above steps, we can ensure that during network reconfiguration, load adjustment and shedding operations can satisfy voltage constraints, thereby achieving service restoration.

4 Distributed Energy Resource Model

During the service restoration process in distribution networks, the integration and utilization of DERs play a crucial role in ensuring system stability and restoration efficiency. Therefore, modeling the output of these resources is an important step in ensuring the successful implementation of service restoration strategies. This section discusses the output characteristics and models of various DERs involved in Eqs. (8) and (9), including WT, PV, ESS, EEV, and controllable loads.

(1) PV output model. The output of PV systems is primarily influenced by solar radiation intensity. The relationship between PV output and solar irradiance is described in Eq. (23).

$$P_{py} = \eta_{py} S C_{py} \tag{23}$$

where, P_{py} is predicted output value of PV at time t; η_{py} is rated PV conversion efficiency; S is area of PV components; C_{py} is radiation intensity of PV components.

(2) WT output model. The output of WT is closely related to the wind speed in the operating environment. The specific output model of WT is described in Eq. (24).

$$\mathrm{P}_{WT} = \begin{cases} 0, & 0 \le v \le v_{ci}, \\ P_N \left(\frac{v - v_{ci}}{v_n - v_{ci}} \right), & v_{ci} \le v \le v_n, \\ P_N, & v_n \le v \le v_{co}, \\ 0, & v > v_{co}. \end{cases} \tag{24}$$

where, P_{WT} is predicted output value of WT at time t; P_N is rated power of WT; v is wind speed at time t; v_{ci} is cut-in wind speed; v_n is rated wind speed; v_{co} is cut-out wind speed.

(3) ESS output model. ESS has the characteristic of stable power output and can maintain voltage and frequency stability in island mode under VF conditions. During network reconfiguration, ESS can balance the power supply and demand, optimize power distribution, and reduce load pressure. However, due to the battery capacity limitations, ESS cannot serve as the main power source for extended periods. In service restoration scenarios, using ESS as a short-term main power source is reasonable because the repair time is generally short. The simplified ESS output model in the normal operating range can be expressed as a linear model [31], as shown in Eq. (25).

$$\begin{cases} 0 \le P_c^{ess}(t) \le \eta_c^{ess} P_{c,\max}^{ess}, \\ 0 \le P_d^{ess}(t) \le \eta_d^{ess} P_{dc,\max}^{ess}, \\ \eta_c^{ess} + \eta_d^{ess} \le 1, \\ E_{ess}(t+1) = E_{ess}(t) + \eta_c^{ess} P_c^{ess}(t) h - \eta_d^{ess} P_d^{ess}(t) h, \\ E_{ess,\min} \le E_{ess}(t) \le E_{ess,\max}. \end{cases} \tag{25}$$

where, $P_c^{ess}(t)$ is charging power of ESS at time t; $P_d^{ess}(t)$ is discharging power of ESS at time t; $P_{c,\max}^{ess}$ is maximum charging power of ESS; $P_{dc,\max}^{ess}$ is maximum discharging power of ESS; η_c^{ess} is charging efficiency of ESS; η_d^{ess} is discharging efficiency of ESS; $E_{ess}(t)$ is remaining battery capacity at the end of time t for ESS; $E_{ess,\min}$ is minimum remaining battery capacity limit of ESS; $E_{ess,\max}$ is maximum remaining battery capacity limit of ESS.

(4) EEV output model. Electric vehicles (EVs) include buses, taxis, government vehicles, private cars, and EEVs. In service restoration, faults often occur rapidly, which requires the quick dispatch of emergency resources. EEV can swiftly respond to system dispatch instructions and promptly participate in fault repair to ensure power supply [32]. EEV is equipped with large-capacity energy storage batteries, with storage capacity and output power significantly greater than ordinary EVs (up to several MVA). In island operation, it can serve as the main power source to maintain voltage and frequency stability. In network reconfiguration, EEV can balance the distribution network load, reduce load pressure, and improve the stability and reliability of the distribution networks. Due to EEV's mobility, it can be flexibly deployed during service restoration, where it is allocated to needed nodes for charging and discharging. The output model of the energy storage battery in EEV is shown in (26).

$$\begin{cases} 0 \le P_c^{eev}(t) \le \eta_c^{eev} P_{c,\max}^{eev}, \\ 0 \le P_d^{eev}(t) \le \eta_d^{eev} P_{dc,\max}^{eev}, \\ \eta_c^{eev} + \eta_d^{ev} \le 1, \\ E_{eev}(t+1) = E_{eev}(t) + \eta_c^{eev} P_c^{eev}(t)\, h - \eta_d^{eev} P_d^{eev}(t)\, h, \\ E_{eev,\min} \le E_{eev}(t) \le E_{eev,\max}. \end{cases} \tag{26}$$

where, $P_c^{eev}(t)$ is charging power of EEV at time t; $P_d^{eev}(t)$ is discharging power of EEV at time t; $P_{c,\max}^{eev}$ is maximum charging power of EEV; $P_{dc,\max}^{eev}$ is maximum discharging power of EEV; η_c^{eev} is charging efficiency of EEV; η_d^{eev} is discharging efficiency of EEV; $E_{eev}(t)$ is remaining battery capacity at the end of time t for EEV; $E_{eev,\min}$ is minimum remaining battery capacity limit of EEV; $E_{eev,\max}$ is maximum remaining battery capacity limit of EEV.

(5) Load characteristic model. Loads are divided into fixed loads and adjustable loads. Fixed loads do not change with time and other factors, as shown in (27). Adjustable loads can be regulated according to a certain proportion, as shown in (28). To determine the weights of different loads, this paper categorizes the loads into three levels—primary, secondary, and tertiary loads—based on their impact on safety and economy after a power outage, with weights of 100, 10, and 1, respectively. Primary loads are prioritized for restoration during distribution network faults, followed by secondary and then tertiary loads.

$$\begin{cases} P_{\text{load},i} = y_i L_i, \\ Q_{\text{load},i} = P_{\text{load},i} \tan\varphi_i. \end{cases} \tag{27}$$

$$\begin{cases} P_{\text{load},j} = (1 - r_i)\, y_i L_i, \\ Q_{\text{load},j} = P_{\text{load},j} \tan\varphi_i. \end{cases} \tag{28}$$

where, L_i is active power demand of node i load; $\tan\varphi_i$ is power factor of load at node i.

5 Service Restoration Model Solution

5.1 Model Solving

The intentional islanding partition and network reconfiguration models described above involve a large number of 0–1 integer variables and quadratic constraints, which constitute a mixed-integer nonlinear programming (MINLP) problem. This paper primarily employs second-order cone relaxation optimization and McCormick relaxation methods to linearize the nonlinear constraints (Eqs. (3), (7), (8), (11), (12), (16), (18), (21) and (22)), thereby transforming the constraints into the following constraints.

$$f = \min \sum_{\forall (i,j)\in\Omega_L} r_{ij} I_{ij}^{sqr} + \sum_{\forall i\in\Omega_n} |U - U_i| \tag{29}$$

$$\sum_{j\in\phi(i)} P_{ji} - \sum_{k\in\phi(i)} P_{ik} - r_{ji} I_{ji}^{sqr} = y_i P_i \tag{30}$$

$$\sum_{j\in\phi(i)} Q_{ji} - \sum_{k\in\phi(i)} Q_{ik} - x_{ji} I_{ji}^{sqr} = y_i Q_i \tag{31}$$

$$\left\| \begin{matrix} 2P_{ij} \\ 2Q_{ij} \\ I_{ij}^{sqr} - U_i^{sqr} \end{matrix} \right\| \le I_{ij}^{sqr} + U_i^{sqr} \tag{32}$$

$$\begin{cases} m_{\overline{y}} = (1-\alpha)\cdot M \\ U_i^{zgr} - U_j^{zgr} \le m_y + 2\left(r_y P_{\overline{y}} + x_y Q_{\overline{y}}\right) - \left(r_{\overline{y}}^2 + x_{\overline{y}}^2\right) I_{\overline{y}}^{zgr} \\ U_i^{zgr} - U_j^{zgr} \ge -m_{\overline{y}} + 2\left(r_y P_{\overline{y}} + x_y Q_{\overline{y}}\right) - \left(r_{\overline{y}}^2 + x_{\overline{y}}^2\right) I_{\overline{y}}^{zgr}. \end{cases} \tag{33}$$

$$f = \min \left[-\sum_{i\in\mathcal{L}} w_i \left(-\gamma_i \alpha_i P_{\text{Load},i} + \gamma_i P_{\text{Load},i}\right) - \sum_{j\notin\mathcal{L}} \gamma_j \gamma_j w_j P_{\text{Load},j} \right] \tag{34}$$

$$\begin{cases} c_{ij}^s \le v^{is}, & \forall ij \in \Omega_l, s \in S \\ c_{ij}^s \le v^{js}, & \forall ij \in \Omega_l, s \in S \\ c_{ij}^2 \ge v^{is} + v^{js} - 1, & \forall ij \in \Omega_l, s \in S \end{cases} \tag{35}$$

$$P_I = -r_i \alpha_i P_{\text{Load},i} + \mathcal{V}_i P_{\text{Load},i} - P_i^{WT} - P_i^{PV} - P_I^{\text{eev}} - P_i^{\text{ess}} \tag{36}$$

$$Q_I = -r_i \alpha_i Q_{\text{Load},i} + \mathcal{V}_i Q_{\text{Load},i} - Q_i^{WT} - Q_i^{PV} - Q_I^{\text{eev}} - Q_i^{\text{ess}} \tag{37}$$

$$\begin{cases} \alpha_i \le \beta_i, & \forall i \in \Omega_b, \\ \alpha_i \le y_i, & \forall i \in \Omega_b, \\ \alpha_i \ge \beta_i + y_i - 1, & \forall i \in \Omega_b. \end{cases} \tag{38}$$

$$U_{\min}^2 \le U_i^{sqr} \le U_{\max}^2 \tag{39}$$

$$0 \le I_{ij}^{sqr} \le z_{ij} I_{\max}^2 \tag{40}$$

$$|P_I| \le P_{I\max} \tag{41}$$

Firstly, to address the quadratic terms I_{ij}^2 and U_i^2 in the nonlinear constraints, this paper introduces new variables I_{ij}^{sqr} and U_i^{sqr}, and defines $I_{ij}^{sqr} = I_{ij}^2$ and $U_i^{sqr} = U_i^2$. To handle the product form of two binary variables in the nonlinear constraints and improve model tractability, these products need to be converted into equivalent linear representations. For constraints (16), (21) and (22), a new variable a_i is introduced by letting $a_i = r_i y_i$. Similarly, for constraint (18), a new variable c_{ij}^s is introduced, where $c_{ij}^s = y^i y^j$, and the McCormick relaxation method is applied for linearization. As a result, Eqs. (3), (7), (8), (16), (18), (21) and (22) are all transformed into linear constraints (29)–(31), and (34)–(38).

However, the nonlinear constraints in (11) and (12) still exist after the aforementioned transformations. To further relax constraint (10), the equality constraint is first converted into an inequality constraint, and then equivalently transformed into the standard second-order cone constraint (32). Regarding (12), to avoid the situation where the voltage magnitudes at both ends of the disconnected branch ij is forced to be equal ($U_i^{sqr} - U_j^{sqr} = 0$), this paper introduces the big-M method, which transforms (12) into (33). In (33), for the network reconfiguration strategy, α is set to Z_{ij}; for the intentional islanding partition strategy, α is set to x_{ij}.

After the aforementioned transformations, both the objective functions and constraints of the model (3)–(22) have been linearized. To clearly describe the algorithmic flow, the model is expressed in a unified and concise form as follows:

$$\min_{x \in \phi} b^T x \tag{42}$$

$$\text{S.t.} \quad Ax \leq b \tag{43}$$

$$\text{Bx} = \text{d} \tag{44}$$

$$\|G_l x\| \leq g_l^T x \quad \forall l = 1, \ldots, m \tag{45}$$

where x represents the optimization variables. For network reconfiguration, $x = \left(z_{si}, Z_{ij}, P_{ij}, Q_{ij}, I_{ij}^{sq_r}, U_i^{sq_r}\right)$, objective functions (42) corresponds to (29), (43) and (44) are the compact forms of the equality and inequality constraints from (4), (5), (9), (10), (13)–(15), (30)–(31), (33) and (45) represents the second-order cone constraint (32). For intentional islanding partition, $x = \left(z_{si}, \gamma_{ks}, c_{ij}^s, X_{ij}, \gamma_j, P_{ij}, Q_{ij}, I_{ij}^{sq_r}, U_i^{sq_r}\right)$, the objective functions (42) corresponds to (34), (43) and (44) are the compact forms of the equality and inequality constraints from (4), (9), (10), (13)–(15), (17), (19), (20), (33), (35), (38) and (45) represents the second-order cone constraint (32). Eqs. (42)–(45) are transformed into MISOCP problems, which can be solved using the CPLEX solver.

5.2 Solving Steps

The flowchart of the service restoration method is presented in Table 2. The basic steps of the service restoration strategy are summarized as follows: After fault isolation, the service restoration strategy is determined by assessing the faulted branch variable, and the respective faulty power outage areas are identified based on the corresponding matrix. Before proceeding with service restoration, it is first necessary to determine whether tie switches exist in the outage area. If tie switches exist, the corresponding switches are taken into account; otherwise, they are disregarded. After these determinations are made, the service restoration strategy for each case is modeled and solved.

Table 2: Flowchart of service restoration method

Service restoration process
01: Input: the parameters of load, branch, DERs, etc.
02: Determine the basic ring matrix $\boldsymbol{M}$ based on the distribution network
03: Identify the faulted branches l
04: Determine the service restoration strategy based on selection criteria
05: Calculate the faulted branch variable x_l^a based on the basic ring matrix $\boldsymbol{M}$
06: If $x_i^a = 0$ (Taking a faulted branch as an example)
07: Select the intentional islanding partition service restoration strategy
08: else
09: Select the network reconfiguration service restoration strategy
10: if the network reconfiguration results do not meet the safety constraints
11: Perform load shedding operations
12: end if
13: Determine the faulty power outage areas using the network hierarchy matrix $\boldsymbol{L}$, branch node matrices $\boldsymbol{F}_N$ and $\boldsymbol{E}_N$, and branch level correlation matrix $\boldsymbol{C}$
14: If tie switch S_i in faulty power outage areas
15: Consider the tie switches as input variables in the model
16: end if
17: Establish the service restoration model (38)–(44)
18: Transform the model into a MISOCP model and solve
19: Return the service restoration results

6 Case Study

6.1 System Parameters

The simulation cases in this paper are conducted using a modified version of the 69-bus distribution system from the American PG&E Company (as shown in Fig. 3). The system comprises 68 branches, 5 tie switches, and 1 primary source. The system's reference voltage is set at 12.66 kV, with a three-phase power rating of 10 MVA and a total network load of 3802.19 + j2694.60 kVA. The branch impedances and node loads can be referenced from reference [30]. In this paper, ESS units are installed at node 2 in the system, and two EEVs are connected at nodes 8 and 16, which can move to different charging connection points based on dispatching commands after the faults occur. WTs and PVs are integrated into the system at nodes, 11, 19, 33, 38, 52, and 65. The loads are categorized into three levels based on their importance and further classified as fixed or adjustable according to power regulation requirements. The specific data used in this case study are presented in Tables 3–6. Among them, the reactive power output of WTs and PVs operates at a fixed power factor, with a power factor (cos ϕ) of 0.95. And this paper considers a single time in fault recovery. Therefore, the outputs of EEV and ESS are set to their maximum output values.

Table 3: ESS and EEV output power parameters

Type	Maximum active power output P_{max}/kW	Maximum reactive power output Q_{max}/kW	Initial capacity ϕ/kW·h
ESS	1100	880	2000
EEV1	330	230	1000
EEV2	650	550	1200

Table 4: Active power output of PV units

Generating units	Integration location	Active power output P_i^{dg}/kW
PV units	11	150
	33	170
	65	220
WT units	19	170
	38	150
	52	220

Table 5: Load importance levels

Importance level	Node
Primary load	6, 12, 18, 35, 37, 42, 51, 57, 62
Secondary load	1, 2, 3, 4, 5, 8, 14, 15, 17, 19, 20, 21, 23, 24, 25, 26, 27, 29, 30, 31, 32, 33, 34, 36, 38, 39, 40, 41, 49, 50, 52, 53, 54, 55, 56, 58, 61, 64, 65, 66, 67, 68, 69
Tertiary load	7, 9, 10, 11, 13, 16, 22, 28, 43, 44, 45, 46, 47, 48, 59, 60, 63

Table 6: Load types

Load type	Node	Adjustment ratio
Adjustable load	11, 22, 38, 44, 50, 63	0.3
Fixed load	Remaining nodes	1

In the network reconfiguration process discussed in the paper, the output of ESS is not considered because the distribution network relies on power supply from the main grid. However, during partitioning islands, the distribution network needs to operate independently, which necessitates taking ESS output into account. In the intentional islanding partition mode, ESS can provide the necessary power support for the distribution network, which ensures the continuity and stability of the power supply in faulty power outage areas. Furthermore, due to the inherent intermittency of WT and PV, these DGs cannot serve as the sole primary power source within an islanded system. Instead, they must be coordinated with ESS, EEV, and other flexible resources to effectively restore power supply.

Unless otherwise stated, all case studies were run with CPLEX 12.10; the runtime reported for each case is 9 s.

6.2 Result Analysis

This paper analyzes four scenarios based on the service restoration strategies outlined in Section 1.

Scenario 1: The faulted branch is 4. Based on the faulted branch variable and decision tree, the network reconfiguration service restoration strategy is adopted. The restoration result is shown as follows: branches 4, 10, 13, 19, and 37 should be disconnected, and tie switches 69 to 73 are closed. EEVs are connected to nodes 9 and 50, and adjustable loads at nodes 22, 44, 50, and 63 participate in regulation. The specific restoration scenario is shown in Fig. 5.

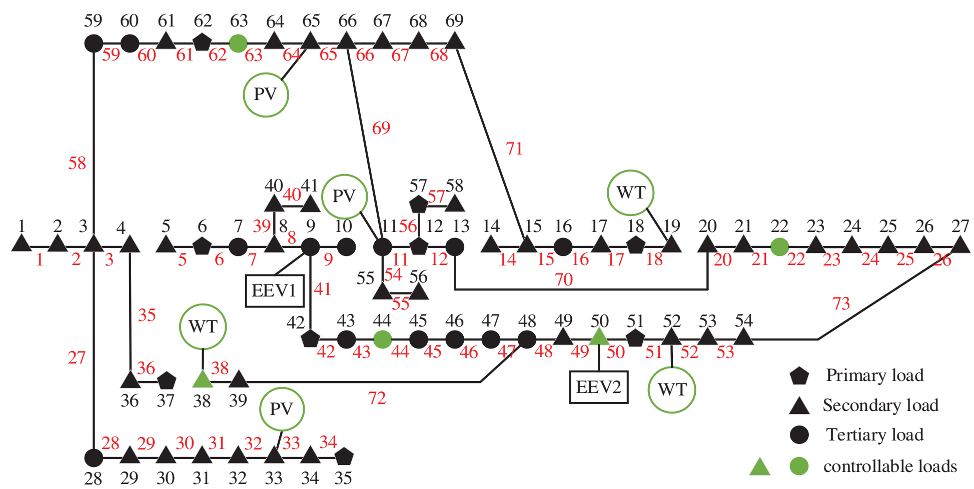

Figure 5: The service restoration situation

Scenario 2: The faulted branch is 27. Based on the faulted branch variable and decision tree, the intentional islanding partition service restoration strategy is adopted. By analyzing the branch incidence matrix, it is determined that there are no tie switches in the faulty power outage area. The restoration result is shown as follows: loads from 28 to 35 are restored through the coordinated power supply of PV and EEV. The specific restoration scenario is shown in Fig. 6.

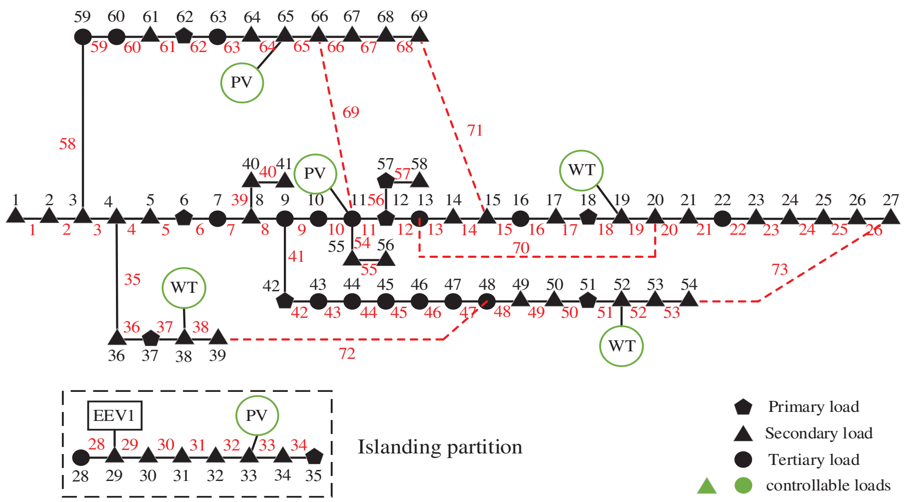

Figure 6: The service restoration situation

Scenario 3: The faulted branches are 20 and 48. Based on the faulted branch variable and decision tree, the intentional islanding partition service restoration strategy is adopted. By analyzing the branch node matrices, it is determined that tie switch 73 exists in the faulty power outage area. Considering the impact of the tie switch, the restoration result is shown as follows: EEVs are connected at nodes 50 and 53, with load regulation at node 50. Through the combined efforts of the EEVs, WT, and tie switch, loads from 49 to 54 are restored. The specific restoration situation is shown in Fig. 7.

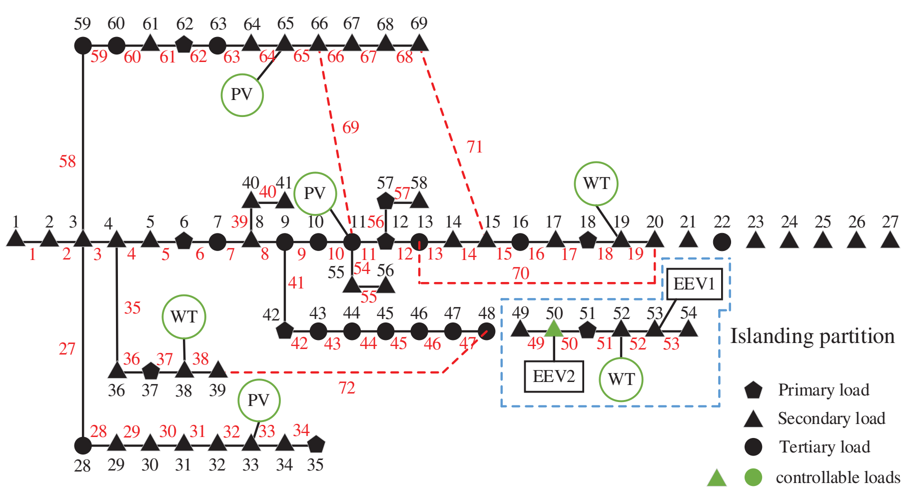

Figure 7: The service restoration situation

Scenario 4: The faulted branches are 59 and 64. Based on the faulted branch variable and decision tree, a combined service restoration strategy that integrates intentional islanding partition with network reconfiguration is adopted. Using the network hierarchy matrix, branch node matrices, and branch level correlation matrix, the island area is identified as nodes 60 to 64, while the remainder constitutes the reconfiguration area. The restoration result is shown as follows: for the island area, since there are no DGs, an EEV is connected to node 60 to supply power, thereby restoring the loads at nodes 60 to 64. For the reconfiguration area, branches 13, 44, 50, and 68 are disconnected, tie switches 69 to 73 are closed, an EEV is connected to node 50, and adjustable loads at nodes 22, 38, 44, and 50 should participate in regulation. The specific restoration scenario is shown in Fig. 8.

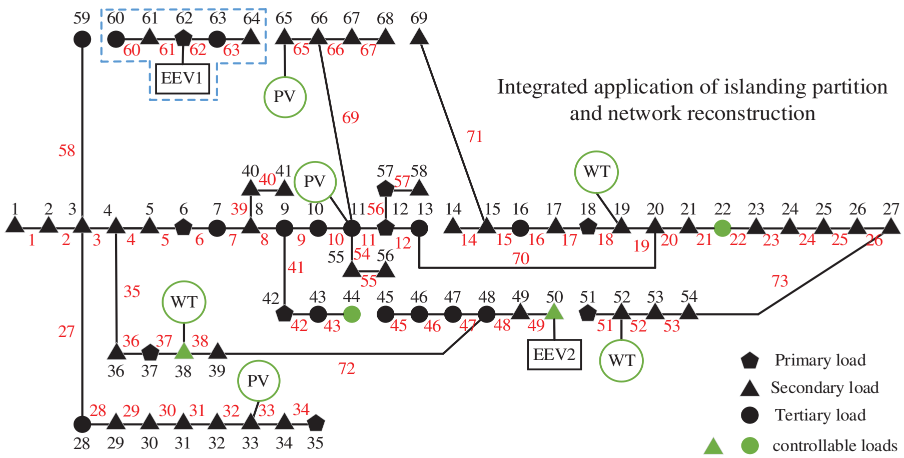

Figure 8: The service restoration situation

Fig. 9 displays the node voltage magnitudes after the service restoration through intentional islanding partition and network reconfiguration using the proposed method in four different scenarios. By comparing each subplot, one can observe that the node voltages after service restoration in each scenario remain within a reasonable operating range, highlighting the effectiveness of the proposed method in ensuring the stability and reliability of the distribution network.

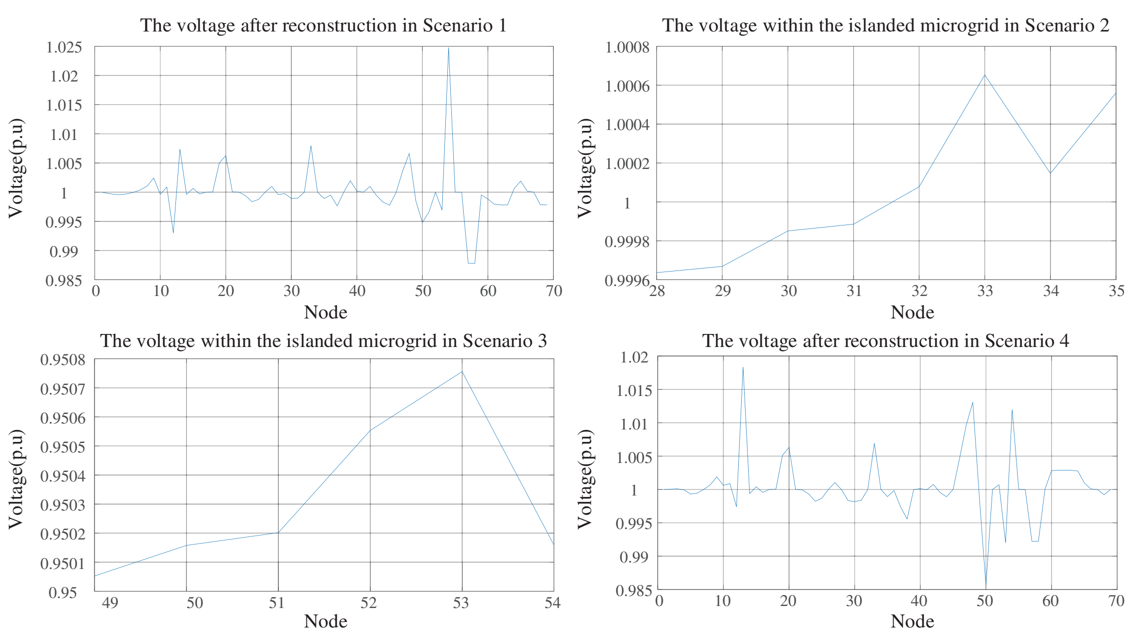

Figure 9: The per unit voltage after service restoration in each scenario

To verify the accuracy of the proposed model, a second-order cone error metric $\Delta_{ij} = \left| P_{ij}^2 + Q_{ij}^2 - I_{ij}^{sq_r} U_i^{sq_r} \right|$ is defined. Taking scenario 1 as an example, Fig. 10 shows the error verification for each branch during the last iteration of the service restoration model using second-order cone relaxation. The overall error metric is controlled within the order of magnitude of 10^{-4}, which meets the requirements of practical applications.

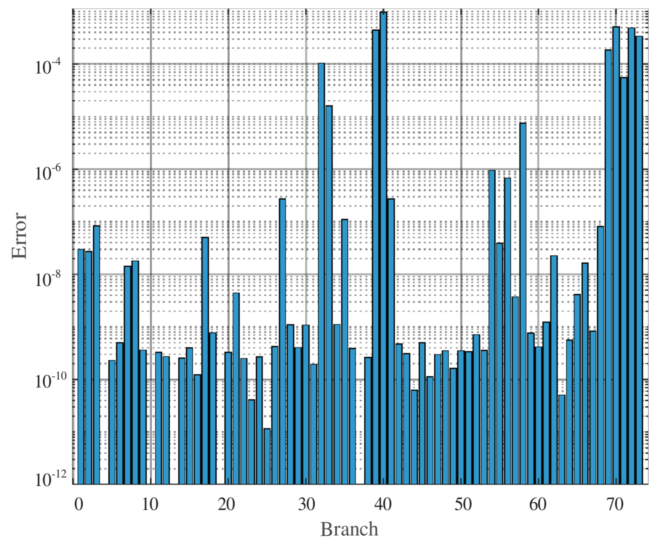

Figure 10: Second-order cone relaxation error verification

For the IEEE 69-bus case, the largest mismatch among all branches after convergence was on the order of 10^{-4} p.u., as shown in Fig. 10. This indicates that the SOC relaxation provides an almost exact representation of the original nonlinear DistFlow equations, and the relaxation gap is negligible for practical applications.

6.3 Comparative Analysis of Service Restoration Involving Distributed Energy Resources

In the process of service restoration, DERs are crucial for improving system efficiency and stability. This section, using the example of a fault on Branch 1, analyzes the specific roles and contributions of resources in service restoration.

6.3.1 Case 1: All DERs Are Considered

Based on the faulted branch variable and decision tree, it is known that when a fault occurs in branch 1, intentional islanding partition strategy is adopted for service restoration, and the role of tie switches should be considered. According to the intentional islanding partition model calculations, the solution indicates that the faulty power outage area is only partitioned into one island for power supply, and the unpowered loads are located at nodes 7–10, 14–16, 40–48, 55–56, and 58, while loads 11, 22, 50, and 63 participate in regulation. EEVs are connected at nodes 50 and 54, and tie switches 69, 70, and 73 are closed. The specific restoration scenario is shown in Fig. 11.

6.3.2 Case 2: Disregarding Controllable Loads

When controllable loads are disregarded, according to the intentional islanding partition model, the solution indicates that the faulty power outage area is only partitioned into one island for power supply, the solution indicates that the faulty power outage area is only partitioned into one island for power supply, and the unpowered loads are located at nodes 7, 14–16, 39, 41, 43–48, and 58. EEVs are connected at nodes 50 and 51, and tie switches 69, 70, and 73 are closed. The specific restoration scenario is shown in Fig. 12.

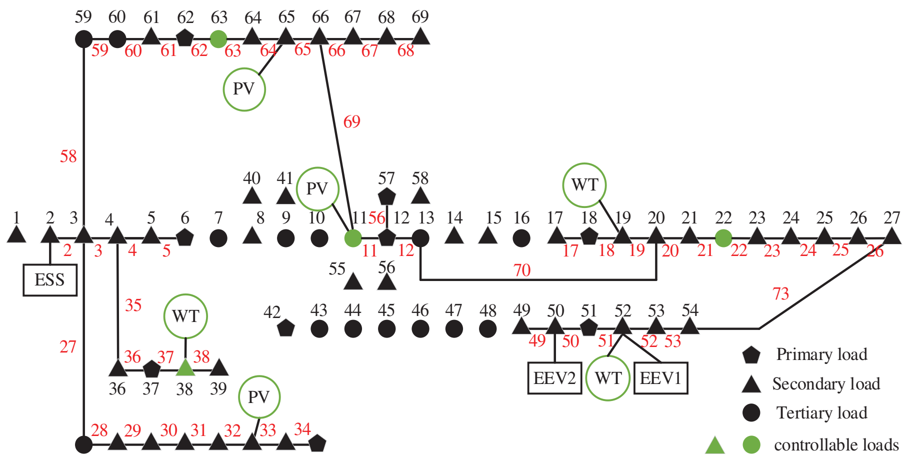

Figure 11: The service restoration situation

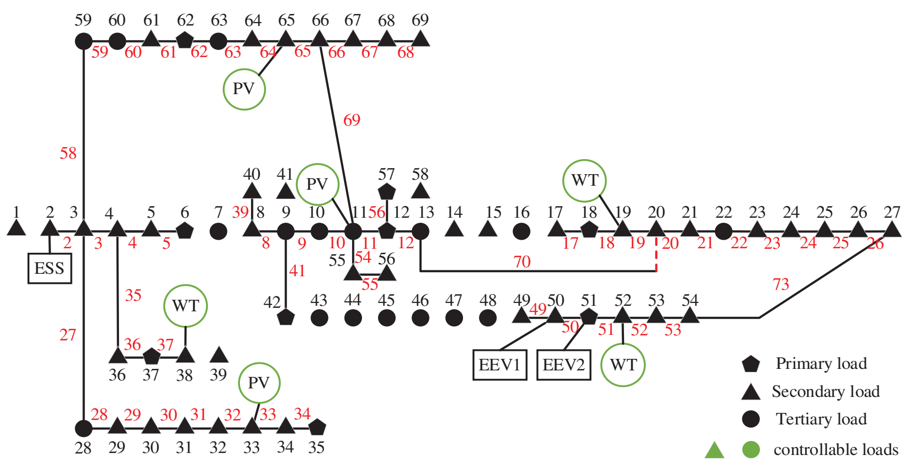

Figure 12: The service restoration situation

6.3.3 Case 3: Disregarding EEV and Controllable Loads

When both EEVs and controllable loads are disregarded, according to the intentional islanding partition model, the solution indicates that the faulty power outage area is partitioned into one island for power supply. In this case, the power outage loads include nodes 7, 14–16, 39, 41, 43–48, 58, and tie switch 69, 70, 73 are closed. The specific restoration scenario is shown in Fig. 13.

6.3.4 Case 4: Disregarding ESS, EEV, and Controllable Loads

In the absence of supporting power sources such as ESS, EEV, and adjustable loads, the output of WT and PV are significantly affected by weather conditions, exhibiting strong uncertainty and volatility. As a result, it is difficult to independently maintain the frequency and voltage stability of the islanded grid. Due to the lack of regulating capabilities from reliable power sources, it becomes challenging to maintain a stable islanded operation status, thereby making it ineffective to achieve power restoration.

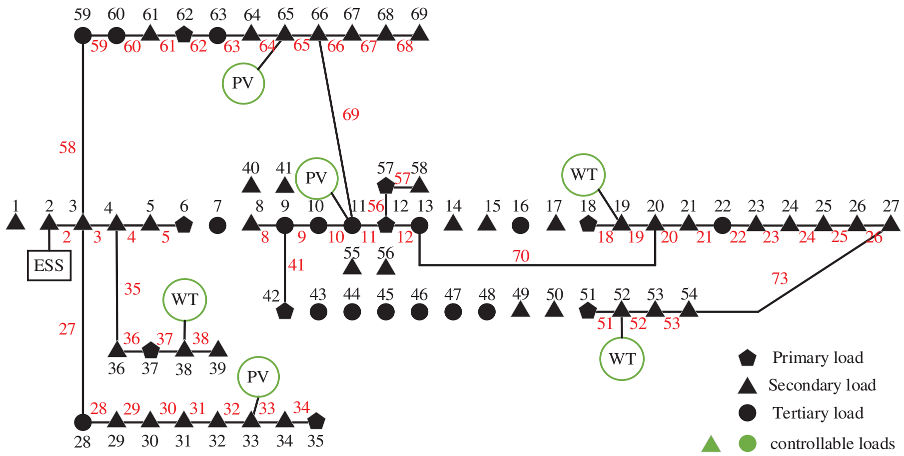

Figure 13: The service restoration situation

The load shedding amounts and the restoration of different levels of loads under the first three scenarios are presented in Table 7. From the table, we can see that the load shedding amounts in the first and second scenarios are similar. However, when adjustable loads are considered, more secondary loads can be restored by regulating tertiary loads. When further considering the scenario without EEVs, the load shedding amounts are 1628.4 kW, mainly due to the large load at node 50, and there is insufficient power supply capacity to restore this load without EEV integration.

Table 7: The service restoration situations in four cases

Case	Load shedding	The restoration level of primary loads	The restoration level of secondary loads	The restoration level of tertiary loads	The range of voltage fluctuations
Case 1	657.51 kW	98.89%	85.62%	37.52%	0.9911~1.0348
Case 2	660.6 kW	100%	85.20%	57.41%	0.9920~1.0499
Case 3	1628.4 kW	100%	51.44%	57.41%	0.9939~1.0350

6.4 Comparison of Service Restoration Strategies

To validate the feasibility of the proposed method, this section uses the IEEE 33-bus system as a case study to compare and analyze the service restoration results of three service restoration methods. Method 1 is the proposed method, which uses the faulted branch variable and decision tree to determine the service restoration strategy. Method 2 ignores the role of tie switches during service restoration. Method 3, as described in reference [19], treats intentional islanding partition and network reconfiguration as two separate problems.

The IEEE 33-bus system has a rated voltage of 12.66 kV and a total load of 3715 + j2300 kVA. Each branch is equipped with a sectional switch, and dashed branches represent tie branches. In the initial network, tie switches are open while other switches are closed. DG1 to DG3 are connected to nodes 5, 12, and 32, respectively, and reactive compensation devices are installed at nodes 16, 24, and 28. Network parameter information is provided in reference [33], the specific parameters of each DG are listed in Table 8, and the levels and weight coefficients of each load are shown in Table 9.

Assuming the faulted branches are branches 9 and 27. The service restoration scenarios for the three methods are shown in Table 10. From Table 10, we can see that Method 2 does not consider the status of tie switches. In the faulty power outage area, only the loads powered by DGs can be restored, while excess loads beyond the DGs remain unpowered. Method 3 considers the role of tie switches based on Method 2. For power outage loads 28 and 29, power can be restored by closing tie switches 37. However, because Method 3 treats intentional islanding partition and network reconfiguration as two separate processes, the service restoration process is divided accordingly. For the outage power from nodes 10–18 caused by the fault on branch 9, restoration follows the principle of prioritizing higher-level loads. Therefore, the DG at node 12 is prioritized to restore power to nodes 12–17, but loads 10–11 and 18 cannot be restored power via tie switches. In contrast, the method proposed in this paper fully integrates intentional islanding partition with network reconfiguration, ensuring that all power outage loads can be restored.

Table 8: Parameters of the DGs

Number	Connection point	Rated capacity
1	5	350
2	12	500
3	32	650

Table 9: Load levels and weighting coefficients

Importance level	Node	Weighting coefficients
Primary load	4, 7, 14, 24, 32	100
Secondary load	2, 6, 8, 15, 16, 17, 22, 23, 27, 29, 33	10
Tertiary load	The remaining nodes	1

Table 10: Fault recovery scenarios of three methods

Method	Load shedding capacity (kW)	Power outage node	Disconnect circuit	Closed circuit
1	0	/	5–6, 13–14, 16–17	7–21, 9–15, 12–22, 18–33, 25–29
2	375	10, 11, 18, 28, 29	10–11, 17–18, 28–29, 29–30	/
3	195	10, 11, 18	5–6, 13–14, 16–17	25–29

6.5 Theoretical Scalability and Computational Performance Analysis

The model's size grows in step with the network because every major decision or physics quantity is indexed by buses or branches already present in the case. Binary decisions come from the reconfiguration switch status z_{ij} and the islanding membership X_{ij}, both branch-indexed; continuous variables cover nodal voltages U_i, bidirectional branch flows P_{ij}, P_{ji}, Q_{ij} and Q_{ji}, DER injections, adjustable-load variables, plus a small number of auxiliaries arising from the linearization and SOC treatment. Constraints are dominated by power balance and flow relations per bus/branch, radiality/topology conditions driven by the basic ring matrix M together with the reconfiguration and islanding count relations, safety limits on voltages/currents/thermal capacities, and per-branch SOC blocks. Taken together, both variables and constraints increase approximately linearly with the numbers of buses, branches, tie switches and modeled DER points.

With binaries fixed, the remaining subproblem is a Second-Order Cone Program as in Section 5 and is solved in polynomial time by interior-point methods; the full model is a MISOCP tackled by branch-and-bound or branch-and-cut, whose worst-case tree size scales rapidly with the number of binary variables.

In practice, tractability is maintained by: hierarchical or two-stage decompositions that choose z_{ij} first then refine flows and voltages with SOC; warm-starts for z_{ij} and X_{ij} from the pre-fault topology and the Section 3.2 decision tree; parallel handling of separable SOC blocks across feeders; and a reduced-order real-time mode that temporarily uses linearized flows and periodically reconciles with the full MISOCP.

7 Conclusion

A flexible matching method for maximum service restoration strategies in active distribution networks with faults is proposed in this paper. The contributions of the proposed method are as follows: (1) By introducing a faulted branch variable and a decision tree, a service restoration strategy that integrates intentional islanding partition with network reconfiguration is proposed. (2) Models for intentional islanding partition and network reconfiguration are established separately. By using second-order cone relaxation optimization and McCormick relaxation methods, the models are transformed into a MISOCP problem. An error analysis of the second-order cone optimization further simplifies the solving process and verifies the feasibility and effectiveness of the model.

Furthermore, we briefly acknowledge the model's simplifications and their potential implications. This study adopts a single-period, deterministic framework; it does not capture the time-coupled dynamics of ESS/EEV (e.g., state-of-charge evolution and mobility), models PV/WT with fixed power factor, and excludes economic objectives. These choices help highlight the "maximum service restoration" mechanism but may overestimate the sustainability of islanded operation and the amount of recoverable load, and they may bias voltage/reactive-power margins and strategy prioritization. Future work will extend the model to a multi-period MISOCP (with SoC dynamics and EEV mobility), incorporate robust/stochastic treatments of renewable and load uncertainty together with cost–constraint co-optimization, and leverage hierarchical decomposition and warm starts to meet near-real-time requirements.

Acknowledgement: Not applicable.

Funding Statement: This work is supported by Natural Science Foundation for Excellent Youth of Hunan Province, China (2023JJ20039).

Author Contributions: The authors confirm contribution to the paper as follows: study conception and design: Yi An and Litao Hong; data collection: Yi An, Zihan Zhang and Chun Chen; analysis and interpretation of results: Chun Chen and Yijia Cao; draft manuscript preparation: Chun Chen, Litao Hong and Yi An. All authors reviewed and approved the final version of the manuscript.

Availability of Data and Materials: Due to the nature of this research, participants of this study did not agree for their data to be shared publicly, so supporting data is not available.

Ethics Approval: Not applicable.

Conflicts of Interest: The authors declare no conflicts of interest.

References

1. Etghani MM, Boodaghi H. Artificial neural networks and taguchi methods for energy systems optimization: a comprehensive review. Energy Eng. 2025;122(11):4385–474. doi:10.32604/ee.2025.070668.
2. Madhiarasan M. Performance analysis of various forecasting models for multi-seasonal global horizontal irradiance forecasting using the India Region dataset. Energy Eng. 2025;122(8):2993–3011. doi:10.32604/ee.2025.068358.

3. Rezaul Karim SM, Hossain MS, Akter K, Sarker D, Kabir MM, Assad M. Impact of dataset size on machine learning regression accuracy in solar power prediction. Energy Eng. 2025;122(8):3041–54. doi:10.32604/ee.2025.066867.
4. Han X, Peng Z, Zhao F, Wan L, Qi W. A novel fault recovery strategy for local power network with high penetrated renewable generation. In: 2023 4th International Conference on Advanced Electrical and Energy Systems (AEES); 2023 Dec 1–3; Shanghai, China. p. 219–24. doi:10.1109/aees59800.2023.10469023.
5. Zidi S, Alaya B, Moulahi T, Al-Shargabi A, El Khediri S. Fault prediction and recovery using machine learning techniques and the HTM algorithm in vehicular network environment. IEEE Open J Intell Transp Syst. 2024;5:132–45. doi:10.1109/ojits.2023.3347484.
6. Sun L, Wang H, Huang Z, Wen F, Ding M. Coordinated islanding partition and scheduling strategy for service restoration of active distribution networks considering minimum sustainable duration. IEEE Trans Smart Grid. 2024;15(6):5539–54. doi:10.1109/tsg.2024.3433603.
7. Kumar V, Kumar HCR, Gupta I, Gupta HO. DG integrated approach for service restoration under cold load pickup. IEEE Trans Power Deliv. 2010;25(1):398–406. doi:10.1109/tpwrd.2009.2033969.
8. Song IK, Jung WW, Kim JY, Yun SY, Choi JH, Ahn SJ. Operation schemes of smart distribution networks with distributed energy resources for loss reduction and service restoration. IEEE Trans Smart Grid. 2013;4(1):367–74. doi:10.1109/tsg.2012.2233770.
9. Li J, Ma XY, Liu CC, Schneider KP. Distribution system restoration with microgrids using spanning tree search. IEEE Trans Power Syst. 2014;29(6):3021–9. doi:10.1109/tpwrs.2014.2312424.
10. Caldon R, Stocco A, Turri R. Feasibility of adaptive intentional islanding operation of electric utility systems with distributed generation. Electr Power Syst Res. 2008;78(12):2017–23. doi:10.1016/j.epsr.2008.06.007.
11. Gautam P, Piya P, Karki R. Resilience assessment of distribution systems integrated with distributed energy resources. IEEE Trans Sustain Energy. 2021;12(1):338–48. doi:10.1109/tste.2020.2994174.
12. Zhao J, Zhang M, Yu H, Ji H, Song G, Li P, et al. An islanding partition method of active distribution networks based on chance-constrained programming. Appl Energy. 2019;242(1):78–91. doi:10.1016/j.apenergy.2019.03.118.
13. Wang S, Wang Z, Liu C, Hou H, Wu X, Gao Q. A review of multi-fault recovery for distribution networks under natural disasters. Procedia Comput Sci. 2022;203:356–61. doi:10.1016/j.procs.2022.07.045.
14. Mishra S, Das D, Paul S. A comprehensive review on power distribution network reconfiguration. Energy Syst. 2017;8(2):227–84. doi:10.1007/s12667-016-0195-7.
15. Jiang H, Liang F, Zhang F. Distribution network based on heuristic search to achieve fault recovery system. Phys Procedia. 2012;24:3–9. doi:10.1016/j.phpro.2012.02.002.
16. Chen S, Hu W, Chen Z. Comprehensive cost minimization in distribution networks using segmented-time feeder reconfiguration and reactive power control of distributed generators. IEEE Trans Power Syst. 2016;31(2):983–93. doi:10.1109/tpwrs.2015.2419716.
17. Nara K, Shiose A, Kitagawa M, Ishihara T. Implementation of genetic algorithm for distribution systems loss minimum re-configuration. IEEE Trans Power Syst. 1992;7(3):1044–51. doi:10.1109/59.207317.
18. Jabr RA, Singh R, Pal BC. Minimum loss network reconfiguration using mixed-integer convex programming. IEEE Trans Power Syst. 2012;27(2):1106–15. doi:10.1109/tpwrs.2011.2180406.
19. Arefifar SA, Mohamed YA-RI, EL-Fouly THM. Comprehensive operational planning framework for self-healing control actions in smart distribution grids. IEEE Trans Power Syst. 2013;28(4):4192–200. doi:10.1109/tpwrs.2013.2259852.
20. Jorge MB, Héctor VO, Miguel LG, Héctor PD. Multi-fault service restoration in distribution networks considering the operating mode of distributed generation. Electr Power Syst Res. 2014;116:67–76. doi:10.1016/j.epsr.2014.05.013.
21. Bansal Y, Sodhi R, Chakrabarti S, Sharma A. A novel two-stage partitioning based reconfiguration method for active distribution networks. IEEE Trans Power Deliv. 2023;38(6):4004–16. doi:10.1109/tpwrd.2023.3298470.
22. Alizadeh M, Jafari-Nokandi M. A bi-level resilience-oriented islanding framework for an active distribution network incorporating electric vehicles parking lots. Electr Power Syst Res. 2023;218:109233. doi:10.1016/j.epsr.2023.109233.

23. Xu R, Zhang C, Zhang D, Dong Z, Yip C. Adaptive robust load restoration via coordinating distribution network reconfiguration and mobile energy storage. IEEE Trans Smart Grid. 2024;15(6):5485–99. doi:10.1109/tsg.2024.3404776.
24. Akrami A, Doostizadeh M, Aminifar F. Optimal reconfiguration of distribution network using μPMU measurements: a data-driven stochastic robust optimization. IEEE Trans Smart Grid. 2020;1(1):420–8. doi:10.1109/tsg.2019.2923740.
25. Chen C, Hong L, Chen Y, Tan Q, Li L, Wang W. Optimal configuration of distributed energy storage considering intending island recovery in faulty distribution networks. Int J Electr Power Energy Syst. 2024;158:109982. doi:10.1016/j.ijepes.2024.109982.
26. Liu W, Liu Y, Yang Y, Xu Q, Dong F. Power restoration model for distribution networks after extreme rainstorm disasters based on electric vehicle travel characteristics. Energy Rep. 2023;9:372–80. doi:10.1016/j.egyr.2022.10.387.
27. Zhao Y, Xiong W, Yuan X, Zou X. A fault recovery strategy of flexible interconnected distribution network with SOP flexible closed-loop operation. Int J Electr Power Energy Syst. 2022;142(1):108360. doi:10.1016/j.ijepes.2022.108360.
28. Chen C, Wang F, Liu B, Cao YJ, Huang C, Dong XZ. Network reconfiguration based on basic ring matrix and improved harmony search algorithm. Autom Electr Power Syst. 2014;38(6):55–60. (In Chinese). doi:10.7500/AEPS20130618011.
29. Wang F, Chen C, Li C, Cao Y, Li Y, Zhou B, et al. A multi-stage restoration method for medium-voltage distribution system with DGs. IEEE Trans Smart Grid. 2017;8(6):2627–36. doi:10.1109/tsg.2016.2532348.
30. Farivar M, Low SH. Branch flow model: relaxations and convexification: part II. IEEE Trans Power Syst. 2013;28(3):2565–72. doi:10.1109/tpwrs.2013.2255318.
31. Ji H, Wang C, Li P, Song G, Wu J. SOP-based islanding partition method of active distribution networks considering the characteristics of DG, energy storage system and load. Energy. 2018;155:312–25. doi:10.1016/j.energy.2018.04.168.
32. Abi-Samra N, McConnach J, Mukhopadhyay S, Wojszczyk B. When the bough breaks: managing extreme weather events affecting electrical power grids. IEEE Power Energy Mag. 2014;12(5):61–5. doi:10.1109/MPE.2014.2331899.
33. Ji H, Wang C, Li P, Ding F, Wu J. Robust operation of soft open points in active distribution networks with high penetration of photovoltaic integration. IEEE Trans Sustain Energy. 2019;10(1):280–9. doi:10.1109/tste.2018.2833545.